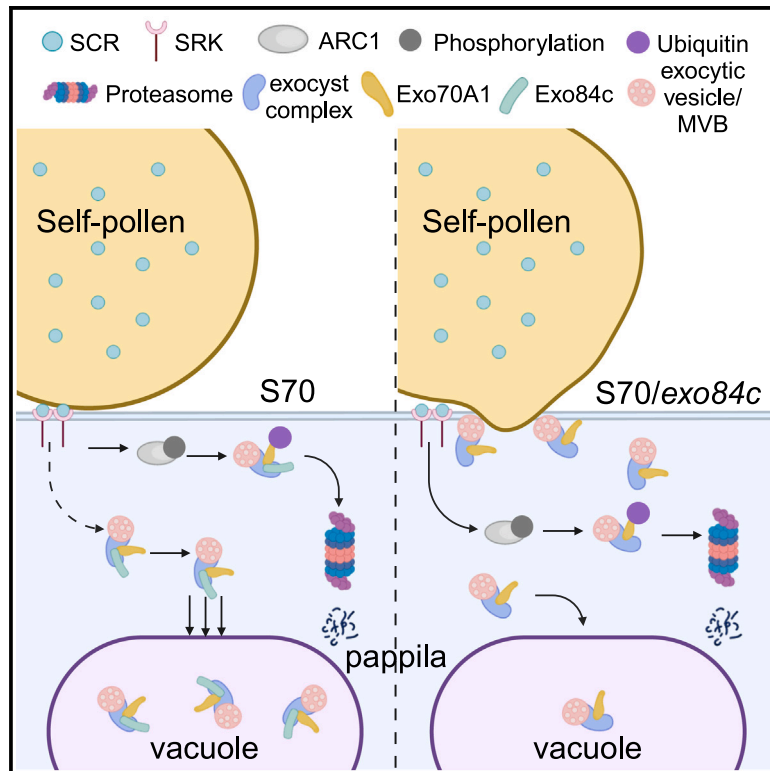


Exo84c-regulated degradation is involved in the normal self-incompatible response in Brassicaceae

Graphical abstract



Authors

Tong Zhang, Kun Wang, Shengwei Dou, Erlin Gao, Patrick J. Hussey, Zongcheng Lin, Pengwei Wang

Correspondence

wangpengwei@mail.hzau.edu.cn

In brief

Many plants have used self-incompatibility to avoid inbreeding and promote outcrossing to maintain genetic diversity. Zhang et al. identify that Exo84c is required for SI response by mediating the vacuolar degradation of exocytic compartments in Brassicaceae species.

Highlights

- The expression of Exo84c is upregulated specifically in SI response
- Suppression of Exo84c results in the breakdown of SI response
- Protein secretion is blocked in SI response
- Exo84c mediates the vacuolar degradation of exocytic compartments in SI response



Article

Exo84c-regulated degradation is involved in the normal self-incompatible response in Brassicaceae

Tong Zhang,^{1,2,4,7} Kun Wang,^{1,3,4,7} Shengwei Dou,^{2,4,5} Erlin Gao,^{1,4} Patrick J. Hussey,⁶ Zongcheng Lin,^{1,4} and Pengwei Wang^{1,3,4,8,*}

¹National Key Laboratory for Germplasm Innovation & Utilization of Horticultural Crops, College of Horticulture and Forestry Sciences, Huazhong Agricultural University, Wuhan 430070, China

²College of Horticulture Science and Engineering, Shandong Agricultural University, Tai'an 271018, China

³College of Life Science and Technology, Huazhong Agricultural University, Wuhan 430070, China

⁴Hubei Hongshan Laboratory, Wuhan 430070, China

⁵National Key Laboratory of Crop Genetic Improvement, Huazhong Agricultural University, Wuhan 430070, China

⁶Department of Biosciences, Durham University, South Road, DH1 3LE Durham, UK

⁷These authors contributed equally

⁸Lead contact

*Correspondence: wangpengwei@mail.hzau.edu.cn

<https://doi.org/10.1016/j.celrep.2024.113913>

SUMMARY

The self-incompatibility system evolves in angiosperms to promote cross-pollination by rejecting self-pollination. Here, we show the involvement of Exo84c in the SI response of both *Brassica napus* and *Arabidopsis*. The expression of Exo84c is specifically elevated in stigma during the SI response. Knocking out Exo84c in *B. napus* and SI *Arabidopsis* partially breaks down the SI response. The SI response inhibits both the protein secretion in papillae and the recruitment of the exocyst complex to the pollen-pistil contact sites. Interestingly, these processes can be partially restored in *exo84c* SI *Arabidopsis*. After incompatible pollination, the turnover of the exocyst-labeled compartment is enhanced in papillae. However, this process is perturbed in *exo84c* SI *Arabidopsis*. Taken together, our results suggest that Exo84c regulates the exocyst complex vacuolar degradation during the SI response. This process is likely independent of the known SI pathway in Brassicaceae to secure the SI response.

INTRODUCTION

Self-incompatibility (SI) has evolved in many angiosperms as a mechanism to avoid self-fertilization and promote cross-pollination, thus ensuring genetic diversity within species and improving their adaptability to a changing environment.¹ The Brassicaceae SI belongs to the sporophytic system, which is determined by the diploid genotype.^{2,3} The SI of Brassicaceae species is activated by the allele-specific recognition of the ligand SCR/SP11 localized in the pollen coat with the receptor kinase SRK enriched in stigma, resulting in the autophosphorylation and activation of SRK.^{4,5} The activated SRK interacts and phosphorylates ARC1, an E3 ligase that targets and degrades downstream self-compatible (SC) components.^{6,7} The exocyst complex subunit, Exo70A1, which regulates exocytic cargo secretion and pollen hydration, is one of the targets of ARC1.⁸ Recently, it has been reported that incompatible response-induced SRK signaling can also recruit FERONIA and result in reactive oxygen species accumulation in the SI stigmas.^{9,10} However, other effectors downstream of the SCR-SRK-mediated signaling pathway remain to be identified.

Protein turnover is regulated by multiple pathways, such as the 26S proteasome-mediated degradation of ubiquitinated proteins (e.g., ARC1 regulated); however, autophagy is another well-known machinery that favors bulk removal of proteins or membranes in a selective way. Recent studies suggested that autophagy is also essential for some key events during plant reproduction, such as pollen tube growth, stigma senescence, and flower receptivity.^{11–13}

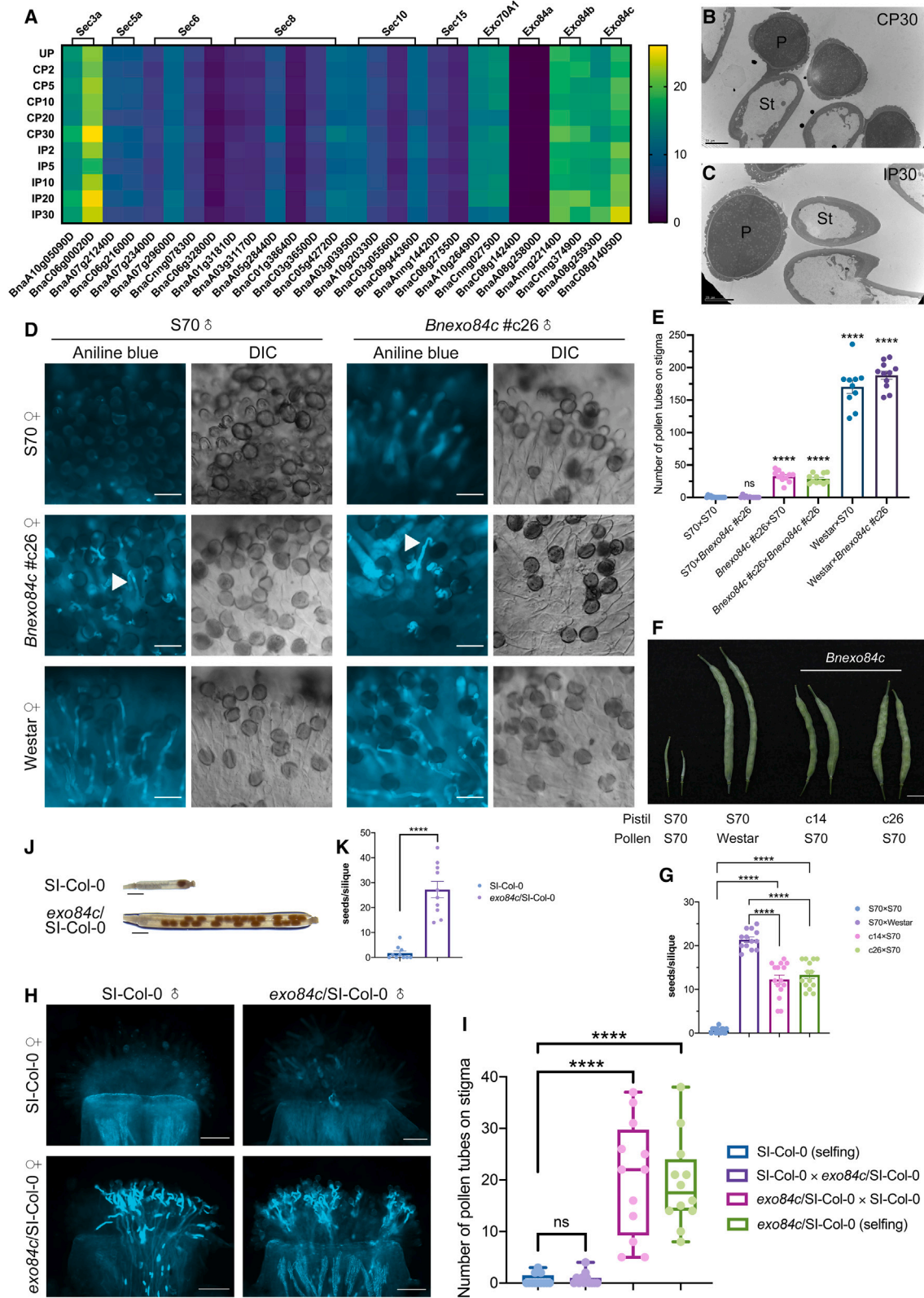
In this context, we investigated whether there are other mechanisms regulating the SI response of Brassicaceae and found that a higher plant-specific exocyst subunit, Exo84c, is required for the SI response. We demonstrate that Exo84c mediates the vacuolar degradation of exocyst compartments or the exocyst complex in both *B. napus* and *Arabidopsis*, and that this mechanism is likely to occur independent of the SCR-SRK-ARC1 machinery.

RESULTS

Exo84c is required for the Brassicaceae SI response

Our previous transcriptome analyses identified differentially expressed genes after compatible or incompatible pollination in





(legend on next page)

B. napus.¹⁴ Further analysis indicated that most of the exocyst complex subunits were expressed at low levels in stigma tissue and exhibited no obvious differences after pollination (Figures 1A–1C and S1A). However, only the expression of Exo84c was specifically elevated after 30 min of incompatible pollination (Figure 1A), indicating that Exo84c may play a role in SI response. Exo84c belongs to the Exo84 family of the exocyst complex; it is specifically found in flowering plants and is phylogenetically distinct from other Exo84 isoforms.¹⁵ We used CRISPR-Cas9 technology to generate BnExo84c loss-of-function mutants in the S70 background, which is an SI cultivar of *B. napus*.¹⁶ There are two copies of BnExo84c genes located in the A08 and C08 chromosomes (Figure S1B), and we have successfully obtained multiple *Bnexo84c* frameshift mutants that are homozygous on the C08 chromosome (Figure S1B). Two independent mutant lines (*Bnexo84c* nos. c14 and c26) were analyzed by immunoblotting using an Arabidopsis Exo84c antibody (Figure S1C). The results show that knocking out one copy of BnExo84c genes leads to a significant reduction in BnExo84c at the protein level (Figure S1D). Self- and reciprocal pollination assays indicated that the mutant of BnExo84c resulted in a partial breakdown of the SI response, with an increased pollen acceptance rate after incompatible pollination (Figures 1D and 1E). In addition, the seed sets were also quantified, and a significant increase was found in the *Bnexo84c* mutants (Figures 1F and 1G), indicating that Exo84c is required for SI response in *B. napus*. As the control, pollen viability of *Bnexo84c* mutants was tested by cross-pollination with a compatible *B. napus* cultivar, Westar,¹⁷ which carries a different S haplotype from S70 (Figures 1D and 1E). These results confirm that the increased pollination efficiency of the *Bnexo84c* mutants is likely attributed to changes in the stigma tissue because their pollen germinated well on Westar stigmas.

Bearing these data in mind, we investigated whether the function of Exo84c in the SI response is conserved in other Brassicaceae species. Because the *Arabidopsis thaliana* Col-0 ecotype is SC due to mutations in both SRK and SCR genes and the lack of an ARC1,^{18–20} transgenic *A. thaliana* Col-0 expressing

AhSCR13-AhSRK13-AhARC1 genes from the SI *A. halleri* (namely SI-Col-0) was used.²¹ This SI-Col-0 system has been tested in many previous studies as a robust and convenient approach for studying SI response in Brassicaceae.^{10,13} We used an Arabidopsis *exo84c* knockout mutant^{12,22} and crossed it with SI-Col-0, and the homozygous progeny (*exo84c*/SI-Col-0) were analyzed. The pollination assay shows that the loss of Exo84c partially breaks down the Arabidopsis SI response, with a significant increase in the number of germinated pollen tubes after SI pollination (Figures 1H and 1I). Furthermore, *exo84c*/SI-Col-0 also set more seeds than SI-Col-0 (Figures 1J and 1K). These results are consistent with our experiments in *B. napus*, indicating that Exo84c plays a conserved role in regulating the SI response in Brassicaceae species.

Protein secretion and exocytosis are inhibited in the SI response

Since the stigma tissue of *B. napus* is too thick for live-cell imaging, the transgenic SI-Col-0 plants were used to study the cellular processes during compatible and incompatible pollination. It is known that substrates required for pollen hydration and pollen-pistil crosstalk need to be transported to pollen from stigmatic papilla through the secretory pathway. Therefore, the secretion marker secGFP²³ driven by the stigma-specific promoter SLR1^{21,24} was introduced into the SI-Col-0 plants to study the secretion activity during the SC and SI responses. When protein secretion is blocked, secGFP accumulates in the endoplasmic reticulum (ER), producing a strong cytoplasmic signal. In contrast, a lower intracellular secGFP signal would indicate an elevated secretion. Our data show that the secGFP fluorescence intensity is significantly reduced upon compatible pollination at 20 min after pollination (MAP), compared with that of unpollination. Moreover, no significant difference is found in the secGFP fluorescence intensity upon incompatible pollination (Figures 2A and 2B). Sometimes, plastids-produced autofluorescence can be distinguished from the real intracellular signal, and do not affect the measurement (Figure S2). The above results indicate that the protein secretion process is activated in

Figure 1. Knocking out the Exo84c gene in *B. napus* and SI Arabidopsis partially breaks the SI response

- (A) mRNA levels (fragments per kilobase of transcript per million mapped reads values) of the exocyst complex subunits at different time points (2, 5, 10, 20, and 30 min) following compatible (CP) and incompatible (IP) pollination of *B. napus*.
- (B and C) Transmission electron micrographs of *B. napus* stigmatic papilla cells 30 min after compatible (B) and incompatible (C) pollination. Compatible pollination pollen grains are adhered to stigmatic papillae and germinated. While in incompatible pollination, pollen grains are not able to adhere to papilla cells. P, pollen; St, stigma. Scale bars, 10 μ m.
- (D) Pollen tube growth on stigmas (indicated with white arrows) of S70, *Bnexo84c* mutants, and Westar at 24 HAP. The SI response of S-70 is partially broken down in *Bnexo84c* mutants. Scale bars, 100 μ m.
- (E) Quantification of pollen germination on stigmas of S70 and *Bnexo84c* plants following manual pollination at 24 HAP (as in D). $n \geq 10$. Error bars represent \pm SEM, and the asterisks represent means that are significantly different at $p < 0.05$ from an ANOVA analysis.
- (F) The size of siliques increased in *Bnexo84c* mutants. Scale bar, 1 cm.
- (G) Quantification of seeds per silique in S-70 and *Bnexo84c* mutants. $n \geq 13$. Error bars represent \pm SEM, and the asterisks represent means that are significantly different at $p < 0.05$ from an ANOVA analysis.
- (H) Images showing pollen tube growth on stigmas of SI-Col-0 and *exo84c*/SI-Col-0. The SI response is partially broken down in *exo84c*/SI-Col-0 mutants. Scale bars, 100 μ m.
- (I) Quantification of pollen germination on stigmas of SI-Col-0 and *exo84c*/SI-Col-0 plants following manual pollination with SI-Col-0 pollen at 24 HAP. $n = 13$. Error bars indicate \pm SEM, and the asterisks represent means that are significantly different at $p < 0.05$ from a 2-tailed Student's *t* test.
- (J) Representative images of cleared siliques used for quantification. Scale bar, 1 mm.
- (K) Quantification of seeds per silique following incompatible pollination in SI-Col-0 and *exo84c*/SI-Col-0. $n = 10$. Error bars indicate \pm SEM, and the asterisks represent means that are significantly different at $p < 0.05$ from a 2-tailed Student's *t* test.

See also Figure S1 and Table S1.

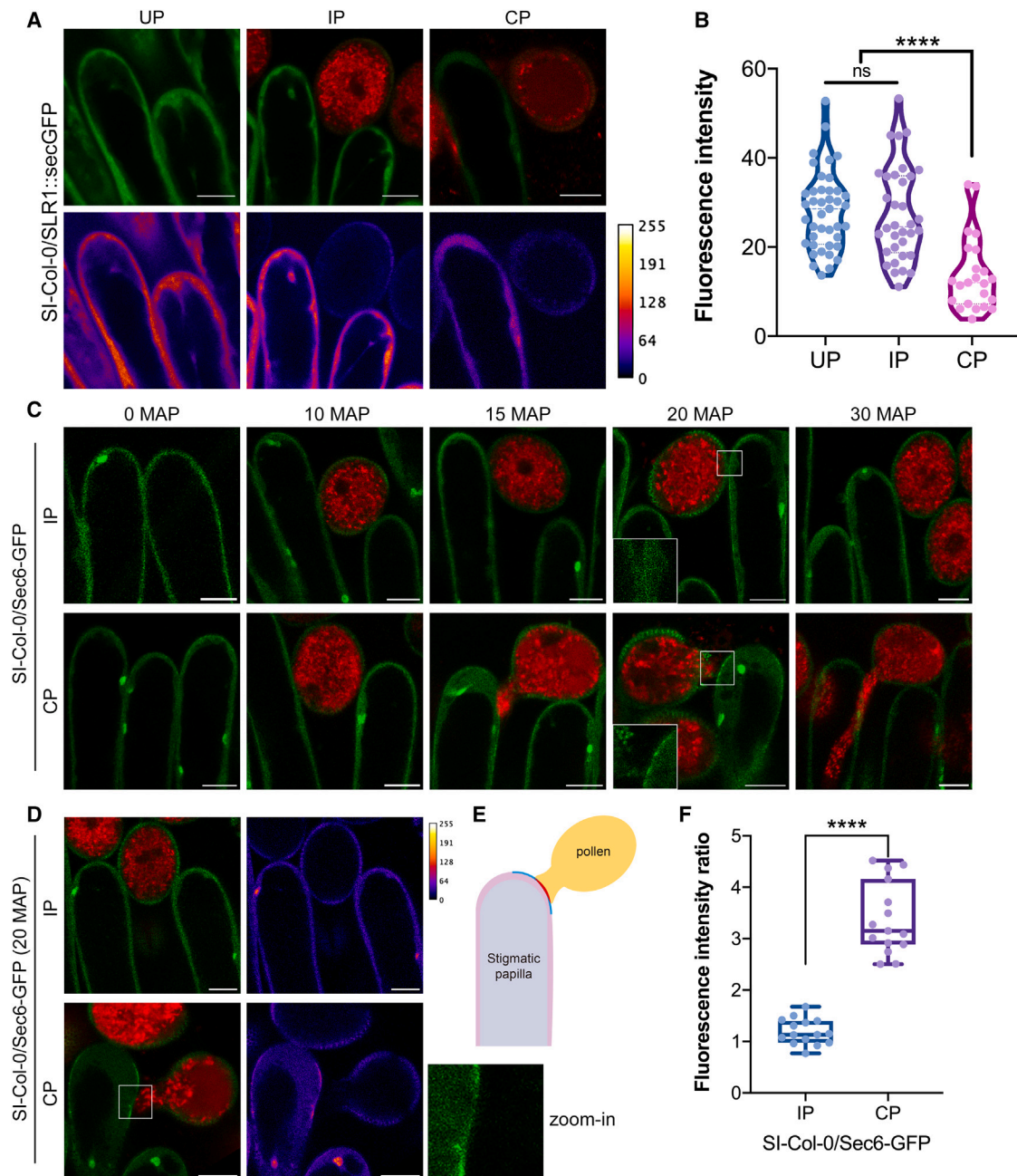


Figure 2. The secretion process is inhibited in the SI response

(A) Representative images showing secGFP signal in papillae of unpollinated (UP), incompatible pollination (IP), and compatible pollination (CP) stigmas. Scale bars, 10 μ m. (Top) Merged images of GFP (papillae) and red fluorescent protein (RFP; pollen) channels. (Bottom) Intensity of GFP fluorescence pseudo-colored to the scale shown (right).

(B) SI response inhibits protein secretion (as measured by the intracellular signal of secGFP) of papillae cells. At least 23 papilla cells from 3 independent stigmas of each sample were used for quantification of secGFP fluorescence intensity. Error bars represent \pm SEM, and the asterisks represent means that are significantly different at $p < 0.05$ from an ANOVA analysis.

(C) Live-cell imaging of the recruitment of Sec6-GFP-labeled exocyst complex to the pollen-stigma contact sites at different time points following incompatible and compatible pollination. Scale bars, 10 μ m. The experiment was repeated 3 times with similar results.

(D) Representative images of the accumulation of Sec6-GFP at the pollen-stigma contact sites at 20 MAP following incompatible and compatible pollination. Scale bars, 10 μ m. Arrows indicate the accumulation of Sec6-GFP signal in (C) and (D). The contact sites of pollen and papilla cells were magnified to show the localization of Sec6-GFP in (C) and (D). (Left) Merged images of GFP (papillae) and RFP (pollen) channels. (Right) Intensity of GFP fluorescence pseudo-colored to the scale shown (right).

(legend continued on next page)

stigmatic papillae during the SC response but is blocked during the SI response.

The exocyst complex is mainly responsible for protein secretion and the delivery of secretory vesicles from the cytoplasm to the plasma membrane.^{15,25} Therefore, we studied the subcellular dynamics of the exocyst complex in stigma tissue after pollination. In yeast and plants, all eight subunits of the exocyst complex can be copurified and remain associated.²⁶ We speculated that any changes in the levels of Exo84c during the SI response may affect the function or activities of the entire exocyst complex. Exo70A1 is one subunit of the exocyst complex and has been reported to be essential for pollen hydration and compatible pollen acceptance.^{8,27} Moreover, Sec6 is known to be a core member of the exocyst complex, which has often been used as a marker for the exocysts.^{28,29} The association of Exo84c to other exocyst subunits was detected using bimolecular fluorescence complementation in *Nicotiana benthamiana*; the results indicate that Exo84c interacts with both Exo70A1 and Sec6 (Figure S3A). In addition, Exo84c-mCh colocalized with GFP-Exo70A1 to the cytoplasm and punctate structures (Figure S3B), supporting the idea that Exo84c and the rest of the exocyst subunits exist in the same protein complex.³⁰

Consequently, we selected Exo70A1 and Sec6 subunits to study the behavior of the exocyst complex after SC and SI pollination. The stable transgenic Arabidopsis Col-0 lines of Sec6p:Sec6-GFP and Exo70A1p:GFP-Exo70A1 were crossed with SI-Col-0, and the resulting SI-Col-0/Sec6-GFP and SI-Col-0/GFP-Exo70A1 lines were further crossed with the *exo84c* mutant, generating *exo84c*/SI-Col-0/Sec6-GFP and *exo84c*/SI-Col-0/GFP-Exo70A1 plants. Pollen germination assays indicate that the introduction of Sec6-GFP or GFP-Exo70A1 into the SI-Col-0 background does not affect their SI response (Figures S4A and S4B), and therefore, they can be used in further functional and cell biology studies.

The localization of Sec6-GFP in papilla cells from SI-Col-0 was examined at different time points following incompatible or compatible pollination, respectively. After 20 min of compatible pollination, Sec6-GFP strongly accumulates at the papilla plasma membrane (PM) where pollen is attached, and the signal disappears as the pollen tubes penetrate the papilla cell at ~30 MAP (Figures 2C, S4C, and S4D). In contrast, no polarized accumulation of Sec6-GFP was observed after incompatible pollination (Figure 2C). The PM accumulation of Sec6-GFP was quantified by calculating the fluorescence intensity ratio between pollen-stigma contact sites and the flanking regions (Figures 2D and 2E), and the results indicate a significant difference between SI and SC responses at 20 MAP (Figure 2F). Moreover, Exo84c-GFP and GFP-Exo70A1 were also found to accumulate at the papilla PM in contact with compatible pollen at 20 MAP (Figures 3, S4E, and S4F). These results reveal dynamic behavior of the exocyst complex after pollination, possibly implicated in exocytosis that is active in compatible pollen germination on the stigmatic papillae.

Exo84c is responsible for inhibiting pollen hydration during the SI response

To investigate why the knock out of Exo84c partially breaks the SI response in Brassicaceae, the behavior of Sec6-GFP in *exo84c*/SI-Col-0 papillae following incompatible pollination was analyzed. Surprisingly, the Sec6-GFP also accumulated at the PM of *exo84c*/SI-Col-0 papilla cells pollinated with incompatible pollen grains. However, such enrichment took much longer to achieve (2 h after pollination [HAP]) (Figures 4A and 4B). As a control, no PM recruitment of Sec6-GFP was found in SI-Col-0 after prolonged pollination.

The blockage of pollen hydration is an early effect of the Brassicaceae SI response,³¹ so we considered whether Exo84c is also involved in this process. The pollen hydration rate was quantified by calculating the length:width ratio at different time points following pollination (a smaller length:width ratio indicates successful hydration). In both *exo84c* and Col-0 plants, the pollen hydration process is completed at ~10 MAP when pollinated with Col-0 pollen (Figures S5A and S5B), indicating that the loss of Exo84c does not affect pollen hydration efficiency after the compatible pollination event. However, the time required for pollen hydration extends to almost 30 min in *exo84c*/SI-Col-0 upon incompatible pollination (Figures 4D, 4E, S5C, and S5D), in agreement with the delayed accumulation of Sec6-GFP at the papilla PM (Figure 4A). In contrast to the SI Arabidopsis, the percentage of hydrated incompatible pollen grains on stigmas of *exo84c*/SI-Col-0 increased significantly (Figure 4F), further indicating that Exo84c is likely to be a positive regulator of the SI response. Taken together, these results imply that active exocytosis and PM recruitment of the exocyst complex is closely associated with compatible pollination. Knocking out Exo84c in the SI-Col-0 background may lead to an incomplete inhibition of exocytosis in papillae during the SI response, which may result in the slow hydration and germination of incompatible pollen.

Exo84c contributes to the vacuolar degradation of exocyst subunits

Because the secretory pathway is essential for determining the SI response, it follows that the activity of the exocyst complex must be tightly controlled. Previous studies have shown that Exo70A1 is degraded through an ARC1-mediated proteasomal pathway, which leads to a block of exocytosis in papilla cells.⁸ However, in *exo84c*/SI-Col-0 plants, although the ARC1-mediated degradation pathway is still active, exocytosis can be partially restored, indicating that there could be other pathways regulating the activity of exocytosis during SI response, which is independent of ARC1. To investigate our hypothesis, the degradation rates of Sec6-GFP (which we are using as a representative member of the exocyst complex) and GFP-Exo70A1 were analyzed by treating plants with cycloheximide (CHX, a protein biosynthesis inhibitor³²). Compared to that in Col-0, the degradation of Sec6-GFP and GFP-Exo70A1 were found to be much

(E) A schematic diagram showing the areas used for the quantification of Sec6-GFP fluorescence intensity ratio. The pollen-stigma contact site is shown in red, and the flanking region is shown in blue.

(F) Quantification of the Sec6-GFP fluorescence intensity ratio in (D). A total of 15 papilla cells from at least 3 stigmas were used for quantification. Error bars indicate \pm SEM, and the asterisks represent means that are significantly different at $p < 0.05$ from a 2-tailed Student's *t* test.

See also Figures S2–S4.

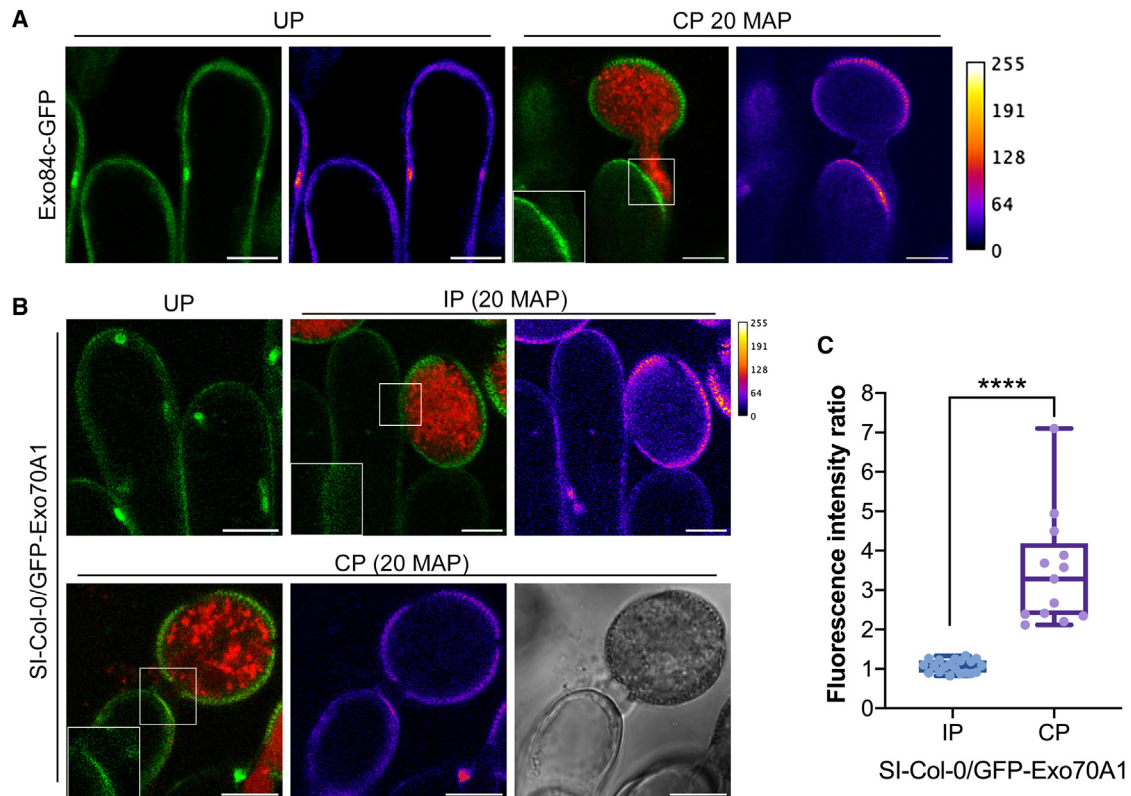


Figure 3. The localization of Exo84c-GFP and GFP-Exo70A1 in papilla cells

(A) Representative images of the accumulation of Exo84c-GFP in the *exo84c* mutant at the pollen-stigma contact sites at 20 MAP following compatible pollination. Scale bars, 10 μ m. The contact sites of pollen and papilla cells were magnified to show the localization of Exo84c-GFP. Images on the left of each panel show the merged images of GFP (papillae) and RFP (pollen) channels. Images on the right of each panel show the intensity of GFP fluorescence pseudo-colored to the scale shown (right).

(B) Representative images of the accumulation of GFP-Exo70A1 at the pollen-stigma contact sites at 20 MAP following incompatible and compatible pollination. Scale bars, 10 μ m.

(C) Quantification of the GFP-Exo70A1 fluorescence intensity in (B). At least 13 papilla cells from 3 stigmas were used for quantification. Error bars indicate \pm SEM, and the asterisk represents means that are significantly different at $p < 0.05$ from a 2-tailed Student's *t* test.

See also [Figure S4](#).

slower in the *exo84c* mutant (Figures 5A, 5B, S6A, and S6B). Therefore, Exo84c is likely to be associated with the degradation of the exocyst subunits. Concanamycin A (conc A) is an inhibitor of vacuolar ATPase, which prevents vacuolar lytic activity. The degradation of Sec6-GFP and GFP-Exo70A1 was inhibited after conc A treatment (Figures 5C, 5D, S6C, and S6D), which indicates that the degradation of Sec6-GFP and GFP-Exo70A1 relies on the vacuolar degradation pathway.^{33,34}

Consequently, we considered whether Exo84c can mediate the vacuolar degradation of exocyst subunits. To test this idea, the vacuolar accumulation of Sec6-GFP was analyzed in papilla cells from SI-Col-0 and *exo84c*/SI-Col-0 plants. Stigma tissues were treated with conc A for at least 6 h before observation, so cargoes that were subject to vacuolar degradation could accumulate and we could quantify their turnover rate from their signal intensity. In the unpollinated stigma, fewer Sec6-GFP-labeled punctate signals were found in the papillae of *exo84c*/SI-Col-0 compared to SI-Col-0 (Figures 5E and 5F), indicating that the loss of Exo84c impairs the default

degradation of Sec6-GFP. Similarly, the vacuolar accumulation of GFP-Exo70A1 was also inhibited in the *exo84c* mutant (Figures S6E and S6F). Since exocytosis is active during compatible pollination, the vacuolar accumulation of Sec6-GFP was then analyzed following compatible and incompatible pollination upon conc A treatment, respectively. At 20 min after compatible pollination, the number of Sec6-GFP-labeled puncta is reduced in papilla cells (Figures 5G and 5H). However, an opposite result was found following incompatible pollination; the number of vacuolar accumulated Sec6-GFP puncta increased significantly in the papilla cells in contact with incompatible pollen than that in papilla cells without pollen (Figures 5I and 5J). These results indicate that the SI response promotes the vacuolar degradation of exocyst subunits. To assess whether Exo84c affects the vacuolar accumulation of Sec6-GFP in SI response, the number of Sec6-GFP-labeled puncta was also quantified in papilla cells of *exo84c*/SI-Col-0 at 20 min after incompatible pollination. Interestingly, in the papilla cells of the *exo84c*/SI-Col-0 mutant, the vacuolar signal of

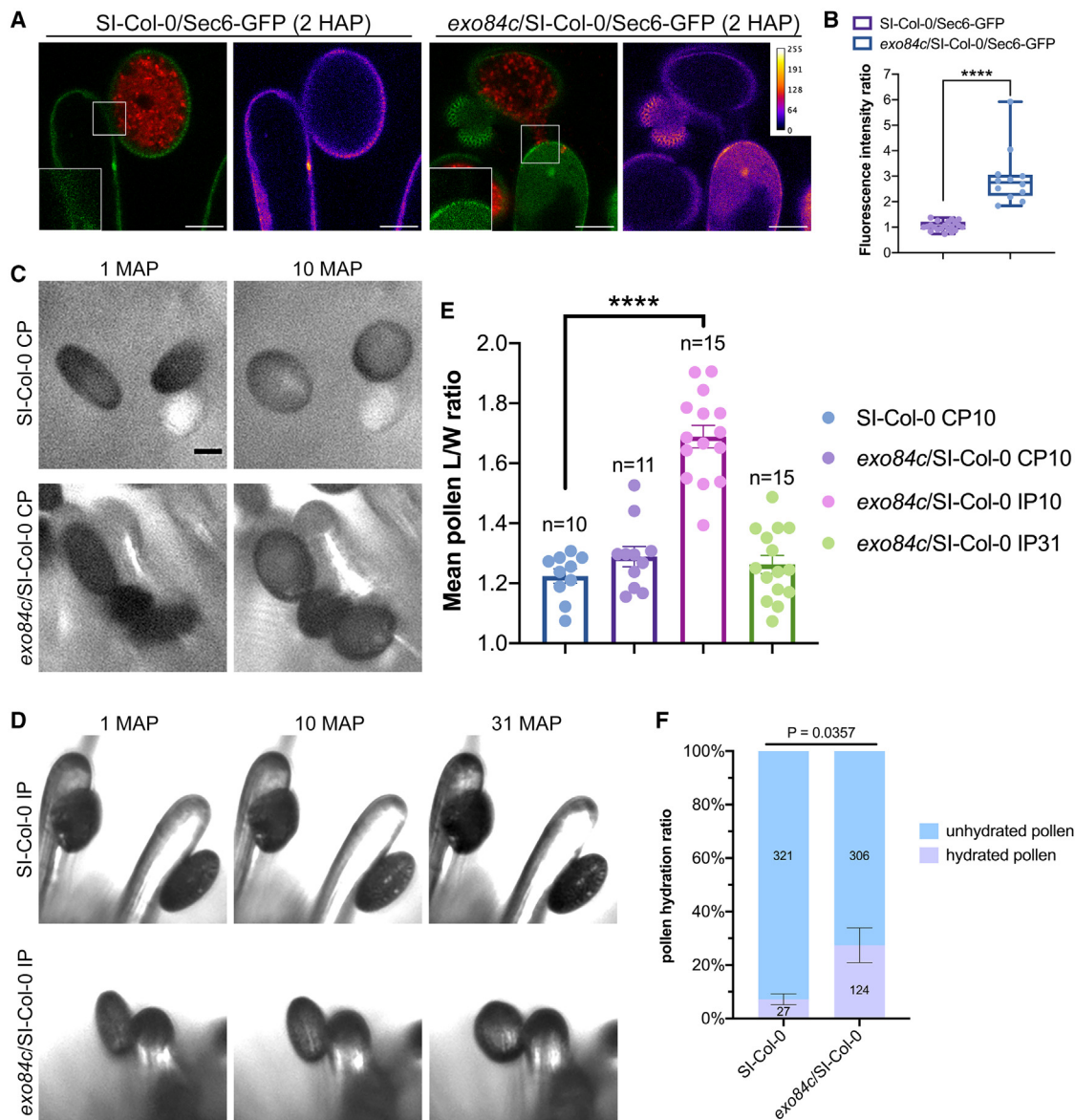


Figure 4. Pollen hydration efficiency is increased in the *exo84c* mutant upon incompatible pollination

(A) In *exo84c*/SI-Col-0 Arabidopsis, Sec6-GFP signal is recruited to the plasma membrane at pollen-pistil contact sites, but at a much slower rate (2 h). Scale bars, 10 μ m. The contact sites of pollen and papilla cells were magnified to show the localization of Sec6-GFP. The left images of each panel show the merged images of GFP (papillae) and RFP (pollen) channels. The right images of each panel show the intensity of GFP fluorescence pseudo-color-coded to the scale shown. (B) Quantification of the Sec6-GFP fluorescence intensity ratio in (A). At least 12 papilla cells from 3 independent stigmas of each sample were used for quantification. Error bars indicate \pm SEM, and the asterisks represent means that are significantly different at $p < 0.05$ from a 2-tailed Student's *t* test. (C and D) Compatible (C) and incompatible (D) pollen hydration on an SI-Col-0 or *exo84c*/SI-Col-0 stigmatic papilla, respectively. Compatible pollen hydration is completed in \sim 10 MAP. Incompatible pollen hydration takes \sim 30 min. Scale bar, 10 μ m. (E) Quantification of the aspect ratio of pollen grains in (C) and (D). Error bars represent \pm SEM, and the asterisks represent means that are significantly different at $p < 0.05$ from an ANOVA analysis. (F) Quantification of hydration ratio of incompatible pollen on SI-Col-0 and *exo84c*/SI-Col-0 stigmas. At least 3 stigmas from each line were used for statistical analysis. A 2-tailed Student's *t* test was performed. CP10, 10 min following compatible pollination. IP10, 10 min following incompatible pollination. IP31, 31 min following incompatible pollination.

See also [Figure S5](#).

Sec6-GFP failed to accumulate after SI pollination (Figures 5K and 5L), indicating that the loss of Exo84c slows down the vacuolar degradation of Sec6-GFP in the SI response.

To further investigate the possible pathway involved in exocyst degradation during SI response, the SI-Col-0 papilla cells were treated with wortmannin, a phosphatidylinositol 3-phosphate

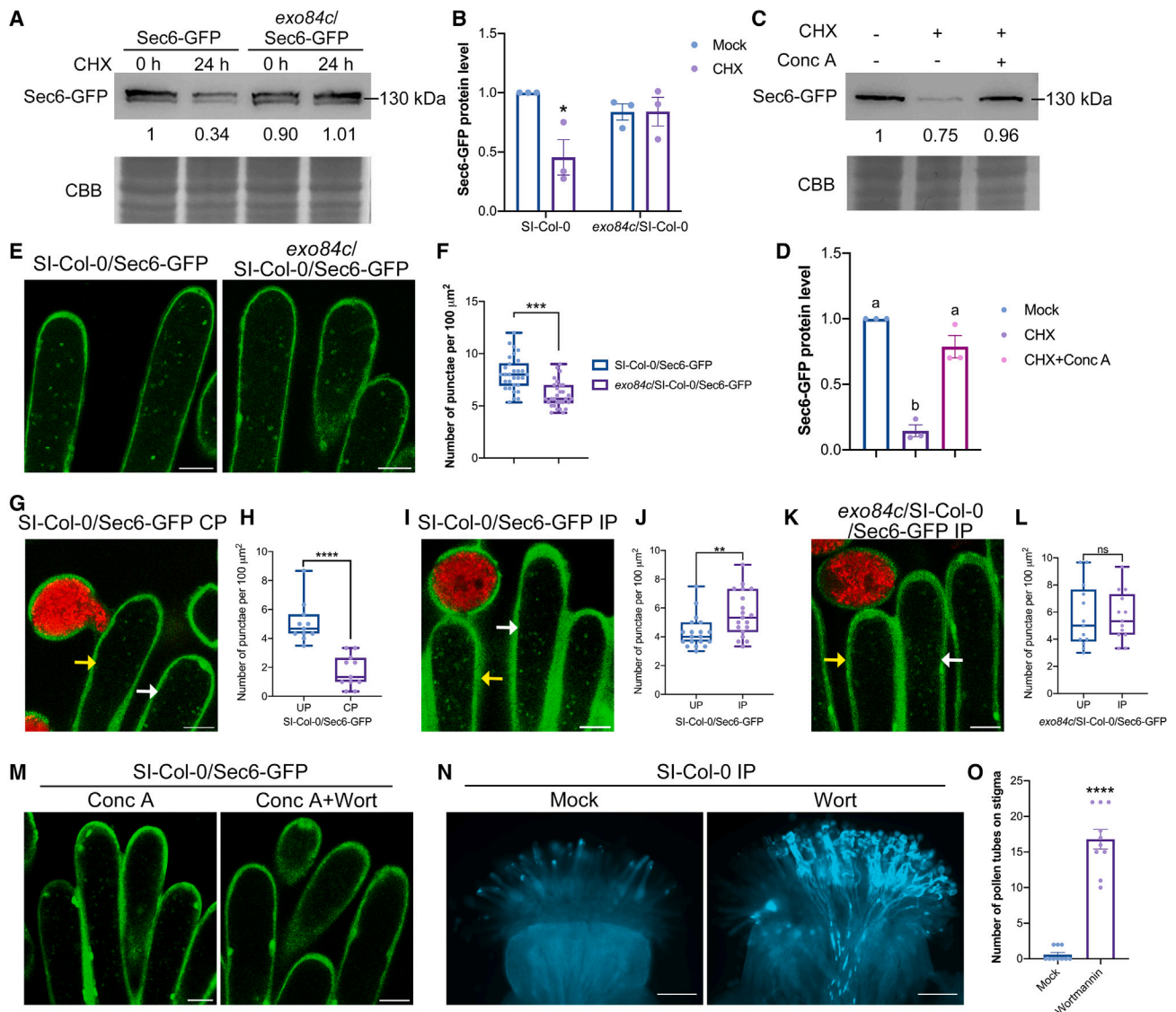


Figure 5. The vacuolar turnover of Sec6-GFP is inhibited in the *exo84c* mutant

(A) An immunoblot assay indicates that the turnover of Sec6-GFP is partially inhibited in the Arabidopsis *exo84c* mutant after CHX treatment. Band intensities were quantified relative to the protein amount of Col-0 at 0 h and are indicated underneath the blot. Coomassie brilliant blue staining was used as a loading control.

(B) Quantification of Sec6-GFP protein levels in the *exo84c* mutant. Three biological repeats were taken for the quantification. Error bars indicate \pm SEM, and the asterisks represent means that are significantly different at $p < 0.05$ from a two-way ANOVA analysis.

(C) An immunoblot assay indicates that the degradation of Sec6-GFP is inhibited after conc A treatment. Band intensities were quantified relative to the Sec6-GFP protein amount without treatment and are indicated underneath the blot. Coomassie brilliant blue staining was used as a loading control.

(D) Quantification of Sec6-GFP protein levels in (C). Three biological repeats were taken for the quantification. Error bars indicate \pm SEM, and the letters represent means that are significantly different at $p < 0.05$ from a one-way ANOVA analysis.

(E) Representative images of the vacuolar accumulated Sec6-GFP signal in unpollinated papilla cells of SI-Col-0 or *exo84c*/SI-Col-0 stigmas upon 6-h conc A treatment. Scale bars, 10 μm .

(F) Quantification of the number of vacuolar accumulated Sec6-GFP punctae in (E) showing an inhibited vacuolar degradation of Sec6-GFP in the *exo84c* mutant. A total of 30 papilla cells from 3 independent stigmas of each sample were used for quantification. Error bars indicate \pm SD, and the asterisks represent means that are significantly different at $p < 0.05$ from a 2-tailed Student's t test.

(G) A representative image of vacuolar accumulated Sec6-GFP in the papilla of SI-Col-0 at 20 min after compatible pollination and 6 h conc A treatment. Scale bar, 10 μm .

(H) The number of vacuolar accumulated Sec6-GFP punctae significantly reduced in papilla cells upon compatible pollination compared to the adjacent unpollinated papillae. A total of 11 papilla cells from 3 independent stigmas were used for quantification. Error bars indicate \pm SD, and the asterisks represent means that are significantly different at $p < 0.05$ from a 2-tailed Student's t test.

(legend continued on next page)

inhibitor that blocks autophagic degradation. There is no vacuolar accumulation of either Sec6-GFP or GFP-Exo70A1 in papillae upon wortmannin treatment (Figures 5M and S6G), and the SI response is also partially broken down in SI-Col-0 with wortmannin treatment (Figures 5N and 5O). Therefore, we suggested that Exo84c-regulated vacuolar degradation following incompatible pollination is likely autophagy related, resulting in a block of exocytosis during the pollen hydration and germination process (Figure 6).

In summary, our study has brought new insight into revealing the underlying mechanism of the SI response. Following incompatible pollination, the SCR-SRK-ARC1 signaling is activated and targets Exo70A1 for proteasomal degradation (Figure 6). In addition, Exo84c likely contributes to the formation of autophagosomes and the selective vacuolar degradation of the exocyst complex through an unknown machinery downstream of the SRK (2). Knocking out Exo84c leads to the inhibition of the vacuolar turnover of the exocyst complex, resulting in a slow exocytic vesicle accumulation at the pollen-stigma contact sites, which consequently promotes pollen hydration and germination. Therefore, in addition to the SCR-SRK-ARC1-mediated proteasomal degradation pathway, Exo84c-mediated degradation may act in parallel to secure the complete incompatible response (Figure 6), whether it is also essential for other sporophytic SI systems is an interesting question for future studies.

DISCUSSION

SCR-SRK-ARC1 is a well-known signaling pathway of the SI response in Brassicaceae. This pathway mediates the proteasomal degradation of downstream components that are required for compatible pollination, including Exo70A1, PLD α 1, and GLO1.^{8,35,36} In addition to the ubiquitin-proteasome system, other protein degradation pathways that regulate protein turnover exist in plants, such as endosomal and autophagic degradation, which takes place in the vacuole.^{33,34} Evidence suggests that protein degradation can be regulated by both the proteasomal and vacuolar turnover systems simultaneously.³⁷ Here, we have identified that Exo84c is a positive regulator of the SI response in both *B. napus* and *A. thaliana*, regulating the vacuolar degradation of exocyst subunits, which in turn leads to the inhibition of incompatible pollen hydration and germination on stigmatic papilla cells.

Previous transmission electron microscopy studies have revealed that vesicles are enriched in papillae following compatible pollination.^{38–40} In addition, mutants or knockdown transgenic plants of some exocyst complex subunits have been reported to be required for compatible pollination under low humidity conditions.²² In our study, by performing a time course in cell imaging, we found that the Sec6-GFP- and GFP-Exo70A1-labeled exocytotic compartments were enriched at the PM of papillae cells after compatible pollination but that similar behaviors were not found during the SI response. These data suggest that the exocytosis is blocked in the SI response, possibly due to the removal of the exocyst complex after incompatible pollination. In contrast, the accumulation of Sec6-GFP at the PM of papilla cells in the *exo84c*/SI-Col-0 mutant is restored, implying that the knockout of Exo84c inhibits the turnover of exocyst subunits. These observations are further confirmed by conc A treatment followed by vacuolar accumulation assays. Autophagy is a well-known process known to regulate the degradation of cytoplasmic cargo and proteins; it is also involved in the SI response of Brassicaceae. Autophagosomes are abundant in papilla cells after incompatible pollination, and knocking out the autophagy genes ATG5 and ATG7 can partially break down the SI response in Arabidopsis.^{13,38–40} Therefore, we suggest that the exocyst subunits and exocytotic compartments are targets for autophagic degradation and that Exo84c is a key regulator in this process, which exists to secure high selectivity.

It is interesting to note that several Exo70 isoforms have been reported to directly interact with ATG8 or autophagy receptors (e.g., NBR1) to mediate the selective autophagic degradation of secretory vesicles.^{41,42} In mammalian cells, the Exo84 subunit is required for nutrient starvation-induced autophagy.⁴³ Our recent results have also suggested that Exo84c interacts with the ER-localized protein VAP27 to mediate the autophagic degradation of other exocyst subunits during stigma senescence.¹² It is possible that Exo84c will interact with autophagy receptors and be recruited to autophagosomes, thereby mediating the degradation of exocyst subunits during the SI response. In addition, other vacuolar degradation pathways exist, involving multivesicular body and exocyst positive organelles. These possibilities are not discussed here since they may also converge with the autophagy pathway at certain conditions.⁴⁴ It would be interesting to understand in future studies

(I) A representative image of vacuolar accumulated Sec6-GFP in the papilla of SI-Col-0 at 20 min after incompatible pollination and 6 h conc A treatment. Scale bar, 10 μ m.

(J) The number of vacuolar accumulated Sec6-GFP punctae increased significantly in papilla cells upon incompatible pollination compared to the adjacent unpollinated papillae from SI-Col-0. A total of 19 papilla cells from 3 independent stigmas were used for quantification. Error bars indicate \pm SD, and the asterisks represent means that are significantly different at $p < 0.05$ from a 2-tailed Student's t test.

(K) A representative image of vacuolar accumulated Sec6-GFP in the papilla of *exo84c*/SI-Col-0 at 20 min after incompatible pollination and 6 h conc A treatment. Scale bar, 10 μ m. White arrows indicate the papilla cells without pollen adhesion in (G), (I), and (K); yellow arrows indicate the papilla cells with compatible pollen germination (G) or papilla cells with incompatible pollen adhesion (I) and (K).

(L) No significant difference is found in the number of vacuolar accumulated Sec6-GFP punctae in papilla cells upon incompatible pollination compared to the adjacent unpollinated papillae from *exo84c*/SI-Col-0. A total of 13 papilla cells from 3 independent stigmas were used for quantification. Error bars indicate \pm SD, and the asterisk represents means that are significantly different at $p < 0.05$ from a 2-tailed Student's t test.

(M) The vacuolar accumulation of Sec6-GFP is blocked in papilla cells of SI-Col-0 upon 500 μ M wortmannin + 33 μ M conc A treatment. Scale bars, 10 μ m.

(N) Images showing pollen tube growth on stigmas of SI-Col-0. The SI response is partially broken down following Wortmannin treatment. Scale bars, 100 μ m.

(O) Quantification of pollen germination on stigmas of SI-Col-0 with or without Wortmannin treatment following manual pollination with SI-Col-0 pollen at 24 HAP. $n = 10$. Error bars indicate \pm SEM, and the asterisks represent means that are significantly different at $p < 0.05$ from a 2-tailed Student's t test.

See also Figure S6.

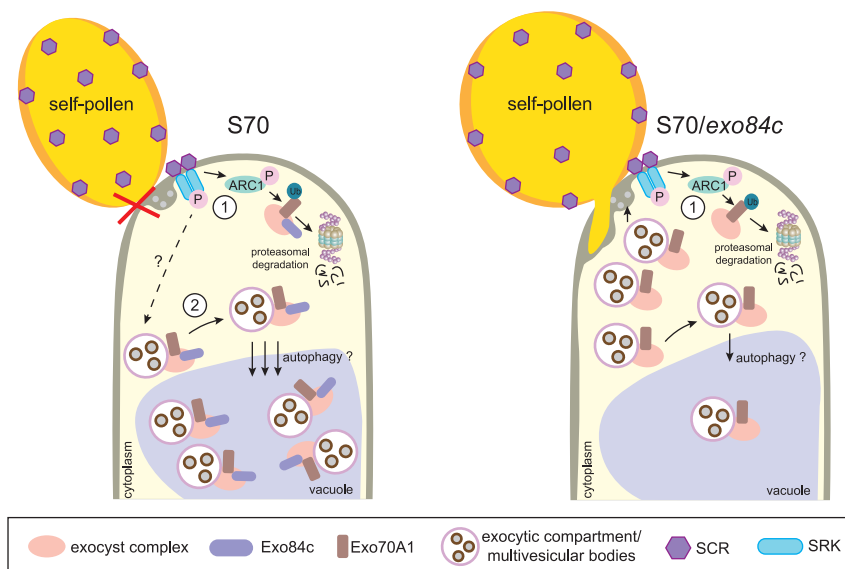


Figure 6. Proposed model for the function of Exo84c in the SI response

(1) SCR-SRK-ARC1 activated proteasomal degradation pathway; (2) Exo84c regulated vacuole/autophagic degradation pathway.

how this Exo84c-mediated vacuolar degradation of exocyst subunits is controlled following the incompatible pollination. Previous studies revealed that Exo70A1 can be phosphorylated by MPK3/4, mediating the compatible pollination.²⁷ It is possible that different posttranslational modifications may be made to Exo84c during compatible or incompatible pollination, which results in the function alteration of Exo84c between exocytosis and vacuolar degradation.

In summary, our data show that there is an elevated level of expression of Exo84c specifically after incompatible pollination in *B. napus* (Figure 1A), and further studies have indicated that Exo84c can directly regulate the degradation of exocyst compartments or the exocyst complex. Therefore, we suggested that these events are essential for the success of the SI response in Brassicaceae species. This mechanism is likely to act in concert with the ARC1-mediated ubiquitin-proteasomal system by inhibiting the hydration and germination of incompatible pollen to secure the SI response and successful cross-pollination.

Limitations of the study

Following incompatible pollination, how Exo84c is associated with the autophagosomes remains to be explained. The cargoes that are transported through exocytic vesicles required for compatible pollen hydration and germination will also need to be elucidated. The signal that induces the autophagic degradation of compatible components during SI response needs to be addressed. We will contribute efforts to reveal the detailed mechanism in the future study.

STAR★METHODS

Detailed methods are provided in the online version of this paper and include the following:

- KEY RESOURCES TABLE
- RESOURCE AVAILABILITY

- Lead contact
- Materials availability
- Data and code availability

● EXPERIMENTAL MODEL AND STUDY PARTICIPANT DETAILS

● METHOD DETAILS

- Transmission Electron Microscopy
- *Brassica napus* transformation
- *Arabidopsis thaliana* transformation
- Production of anti-Exo84c polyclonal antibodies
- Protein extraction and immunoblot analysis
- Chemical treatment
- Pollination assay and silique clearing
- Pollen hydration assay
- Confocal microscopy and image analysis

● QUANTIFICATION AND STATISTICAL ANALYSIS

SUPPLEMENTAL INFORMATION

Supplemental information can be found online at <https://doi.org/10.1016/j.celrep.2024.113913>.

ACKNOWLEDGMENTS

We thank Dr Patrick Duckney (Durham University) for providing the Lat52:RFP-HDEL Arabidopsis line, and Professor Qiaohong Duan (Shandong Agricultural University) for providing some experimental materials. We thank Dr Jianbo Cao and the Public Laboratory of Electron Microscopy, Huazhong Agricultural University. The project was supported by NSFC grants (92254307, 32300301, and 32261160371), Fundamental Research Funds for the Central Universities (2662023PY011), Young Scientist Fostering Funds for the National Key Laboratory for Germplasm Innovation and Utilization of Horticultural Crops (Horti-PY-2023-001), and a China Postdoctoral Science Foundation (2021M691166) grant to P.W. and T.Z.

AUTHOR CONTRIBUTIONS

P.W. conceived and supervised the project. T.Z. and K.W. performed most of the experiments. T.Z. wrote and edited the manuscript with P.W., Z.L., and

P.J.H. S.D. helped with the molecular cloning and transgenic plant generation. E.G. contributed to the data interpretation and result discussion throughout the project.

DECLARATION OF INTERESTS

The authors declare no competing interests.

Received: August 17, 2023

Revised: January 11, 2024

Accepted: February 19, 2024

REFERENCES

- De Nettancourt, D., and De Nettancourt, D. (2001). Incompatibility and Incongruity in Wild and Cultivated Plants.
- Goring, D.R., Bosch, M., and Franklin-Tong, V.E. (2023). Contrasting self-recognition rejection systems for self-incompatibility in Brassica and Papaver. *Curr. Biol.* 33, R530–R542. <https://doi.org/10.1016/j.cub.2023.03.037>.
- Takayama, S., and Isogai, A. (2005). Self-incompatibility in plants. *Annu. Rev. Plant Biol.* 56, 467–489. <https://doi.org/10.1146/annurev.arplant.56.032604.144249>.
- Takayama, S., Shimosato, H., Shiba, H., Funato, M., Che, F.S., Watanabe, M., Iwano, M., and Isogai, A. (2001). Direct ligand-receptor complex interaction controls Brassica self-incompatibility. *Nature* 413, 534–538. <https://doi.org/10.1038/35097104>.
- Kachroo, A., Schopfer, C.R., Nasrallah, M.E., and Nasrallah, J.B. (2001). Allele-specific receptor-ligand interactions in Brassica self-incompatibility. *Science* 293, 1824–1826. <https://doi.org/10.1126/science.1062509>.
- Stone, S.L., Anderson, E.M., Mullen, R.T., and Goring, D.R. (2003). ARC1 is an E3 ubiquitin ligase and promotes the ubiquitination of proteins during the rejection of self-incompatible Brassica pollen. *Plant Cell* 15, 885–898. <https://doi.org/10.1105/tpc.009845>.
- Abhinandan, K., Sankaranarayanan, S., Macgregor, S., Goring, D.R., and Samuel, M.A. (2022). Cell-cell signaling during the Brassicaceae self-incompatibility response. *Trends Plant Sci.* 27, 472–487. <https://doi.org/10.1016/j.tplants.2021.10.011>.
- Samuel, M.A., Chong, Y.T., Haasen, K.E., Aldea-Brydges, M.G., Stone, S.L., and Goring, D.R. (2009). Cellular pathways regulating responses to compatible and self-incompatible pollen in Brassica and Arabidopsis stigmas intersect at Exo70A1, a putative component of the exocyst complex. *Plant Cell* 21, 2655–2671. <https://doi.org/10.1105/tpc.109.069740>.
- Zhang, L., Huang, J., Su, S., Wei, X., Yang, L., Zhao, H., Yu, J., Wang, J., Hui, J., Hao, S., et al. (2021). FERONIA receptor kinase-regulated reactive oxygen species mediate self-incompatibility in Brassica rapa. *Curr. Biol.* 31, 3004–3016.e4. <https://doi.org/10.1016/j.cub.2021.04.060>.
- Huang, J., Yang, L., Yang, L., Wu, X., Cui, X., Zhang, L., Hui, J., Zhao, Y., Yang, H., Liu, S., et al. (2023). Stigma receptors control intraspecies and interspecies barriers in Brassicaceae. *Nature* 614, 303–308. <https://doi.org/10.1038/s41586-022-05640-x>.
- Yan, H., Zhuang, M., Xu, X., Li, S., Yang, M., Li, N., Du, X., Hu, K., Peng, X., Huang, W., et al. (2023). Autophagy and its mediated mitochondrial quality control maintain pollen tube growth and male fertility in Arabidopsis. *Autophagy* 19, 768–783. <https://doi.org/10.1080/15548627.2022.2095838>.
- Zhang, T., Li, Y., Li, C., Zang, J., Gao, E., Kroon, J.T., Qu, X., Hussey, P.J., and Wang, P. (2023). Exo84c interacts with VAP27 to regulate exocytotic compartment degradation and stigma senescence. *Nat. Commun.* 14, 4888. <https://doi.org/10.1038/s41467-023-40729-5>.
- Macgregor, S.R., Lee, H.K., Nelles, H., Johnson, D.C., Zhang, T., Ma, C., and Goring, D.R. (2022). Autophagy is required for self-incompatible pollen rejection in two transgenic Arabidopsis thaliana accessions. *Plant Physiol.* 188, 2073–2084. <https://doi.org/10.1093/plphys/kiac026>.
- Zhang, T., Gao, C., Yue, Y., Liu, Z., Ma, C., Zhou, G., Yang, Y., Duan, Z., Li, B., Wen, J., et al. (2017). Time-Course Transcriptome Analysis of Compatible and Incompatible Pollen-Stigma Interactions in Brassica napus L. *Front. Plant Sci.* 8, 682. <https://doi.org/10.3389/fpls.2017.00682>.
- Chong, Y.T., Gidda, S.K., Sanford, C., Parkinson, J., Mullen, R.T., and Goring, D.R. (2010). Characterization of the Arabidopsis thaliana exocyst complex gene families by phylogenetic, expression profiling, and subcellular localization studies. *New Phytol.* 185, 401–419. <https://doi.org/10.1111/j.1469-8137.2009.03070.x>.
- Chen, F., Yang, Y., Li, B., Liu, Z., Khan, F., Zhang, T., Zhou, G., Tu, J., Shen, J., Yi, B., et al. (2019). Functional Analysis of M-Locus Protein Kinase Revealed a Novel Regulatory Mechanism of Self-Incompatibility in Brassica napus L. *Int. J. Mol. Sci.* 20, 3303. <https://doi.org/10.3390/ijms20133303>.
- Okamoto, S., Odashima, M., Fujimoto, R., Sato, Y., Kitashiba, H., and Nishio, T. (2007). Self-compatibility in Brassica napus is caused by independent mutations in S-locus genes. *Plant J.* 50, 391–400. <https://doi.org/10.1111/j.1365-3113X.2007.03058.x>.
- Boggs, N.A., Nasrallah, J.B., and Nasrallah, M.E. (2009). Independent S-locus mutations caused self-fertility in Arabidopsis thaliana. *PLoS Genet.* 5, e1000426. <https://doi.org/10.1371/journal.pgen.1000426>.
- Tsuchimatsu, T., Suwabe, K., Shimizu-Inatsugi, R., Isokawa, S., Pavlidis, P., Städler, T., Suzuki, G., Takayama, S., Watanabe, M., and Shimizu, K.K. (2010). Evolution of self-compatibility in Arabidopsis by a mutation in the male specificity gene. *Nature* 464, 1342–1346. <https://doi.org/10.1038/nature08927>.
- Indriolo, E., Tharmapalan, P., Wright, S.I., and Goring, D.R. (2012). The ARC1 E3 ligase gene is frequently deleted in self-compatible Brassicaceae species and has a conserved role in Arabidopsis lyrata self-pollen rejection. *Plant Cell* 24, 4607–4620. <https://doi.org/10.1105/tpc.112.104943>.
- Zhang, T., Zhou, G., Goring, D.R., Liang, X., Macgregor, S., Dai, C., Wen, J., Yi, B., Shen, J., Tu, J., et al. (2019). Generation of Transgenic Self-Incompatible Arabidopsis thaliana Shows a Genus-Specific Preference for Self-Incompatibility Genes. *Plants* 8, 570. <https://doi.org/10.3390/plants8120570>.
- Safavian, D., Zayed, Y., Indriolo, E., Chapman, L., Ahmed, A., and Goring, D.R. (2015). RNA Silencing of Exocyst Genes in the Stigma Impairs the Acceptance of Compatible Pollen in Arabidopsis. *Plant Physiol.* 169, 2526–2538. <https://doi.org/10.1104/pp.15.00635>.
- Batoko, H., Zheng, H.Q., Hawes, C., and Moore, I. (2000). A rab1 GTPase is required for transport between the endoplasmic reticulum and golgi apparatus and for normal golgi movement in plants. *Plant Cell* 12, 2201–2218. <https://doi.org/10.1105/tpc.12.11.2201>.
- Foster, E., Levesque-Lemay, M., Schneiderman, D., Albani, D., Scherthaner, J., Routly, E., and Robert, L.S. (2005). Characterization of a gene highly expressed in the Brassica napus pistil that encodes a novel proline-rich protein. *Sex. Plant Reprod.* 17, 261–267. <https://doi.org/10.1007/s00497-004-0236-6>.
- Vukašinić, N., and Žárský, V. (2016). Tethering Complexes in the Arabidopsis Endomembrane System. *Front. Cell Dev. Biol.* 4, 46. <https://doi.org/10.3389/fcell.2016.00046>.
- Mei, K., Li, Y., Wang, S., Shao, G., Wang, J., Ding, Y., Luo, G., Yue, P., Liu, J.J., Wang, X., et al. (2018). Cryo-EM structure of the exocyst complex. *Nat. Struct. Mol. Biol.* 25, 139–146. <https://doi.org/10.1038/s41594-017-0016-2>.
- Jamshed, M., Sankaranarayanan, S., Abhinandan, K., and Samuel, M.A. (2020). Stigma Receptivity Is Controlled by Functionally Redundant MAPK Pathway Components in Arabidopsis. *Mol. Plant* 13, 1582–1593. <https://doi.org/10.1016/j.molp.2020.08.015>.
- Fendrych, M., Synek, L., Pecenková, T., Drdová, E.J., Sekeres, J., de Rycke, R., Nowack, M.K., and Žárský, V. (2013). Visualization of the exocyst complex dynamics at the plasma membrane of Arabidopsis thaliana. *Mol. Biol. Cell* 24, 510–520. <https://doi.org/10.1091/mbc.E12-06-0492>.

29. Wu, J., Tan, X., Wu, C., Cao, K., Li, Y., and Bao, Y. (2013). Regulation of cytokinesis by exocyst subunit SEC6 and KEULE in *Arabidopsis thaliana*. *Mol. Plant* 6, 1863–1876. <https://doi.org/10.1093/mp/sst082>.
30. Zárský, V., Kulich, I., Fendrych, M., and Pečenková, T. (2013). Exocyst complexes multiple functions in plant cells secretory pathways. *Curr. Opin. Plant Biol.* 16, 726–733. <https://doi.org/10.1016/j.pbi.2013.10.013>.
31. Chapman, L.A., and Goring, D.R. (2010). Pollen-pistil interactions regulating successful fertilization in the Brassicaceae. *J. Exp. Bot.* 61, 1987–1999. <https://doi.org/10.1093/jxb/erq021>.
32. Liu, Y., Zhang, C., Wang, D., Su, W., Liu, L., Wang, M., and Li, J. (2015). EBS7 is a plant-specific component of a highly conserved endoplasmic reticulum-associated degradation system in *Arabidopsis*. *Proc. Natl. Acad. Sci. USA* 112, 12205–12210. <https://doi.org/10.1073/pnas.1511724112>.
33. Gao, C., Zhuang, X., Shen, J., and Jiang, L. (2017). Plant ESCRT Complexes: Moving Beyond Endosomal Sorting. *Trends Plant Sci.* 22, 986–998. <https://doi.org/10.1016/j.tplants.2017.08.003>.
34. Qi, H., Xia, F.N., and Xiao, S. (2021). Autophagy in plants: Physiological roles and post-translational regulation. *J. Integr. Plant Biol.* 63, 161–179. <https://doi.org/10.1111/jipb.12941>.
35. Sankaranarayanan, S., Jamshed, M., and Samuel, M.A. (2015). Degradation of glyoxalase I in *Brassica napus* stigma leads to self-incompatibility response. *Nat. Plants* 1, 15185. <https://doi.org/10.1038/nplants.2015.185>.
36. Scandola, S., and Samuel, M.A. (2019). A Flower-Specific Phospholipase D Is a Stigmatic Compatibility Factor Targeted by the Self-Incompatibility Response in *Brassica napus*. *Curr. Biol.* 29, 506–512.e4. <https://doi.org/10.1016/j.cub.2018.12.037>.
37. Xia, F.N., Zeng, B., Liu, H.S., Qi, H., Xie, L.J., Yu, L.J., Chen, Q.F., Li, J.F., Chen, Y.Q., Jiang, L., and Xiao, S. (2020). SINAT E3 Ubiquitin Ligases Mediate FREE1 and VPS23A Degradation to Modulate Abscisic Acid Signaling. *Plant Cell* 32, 3290–3310. <https://doi.org/10.1105/tpc.20.00267>.
38. Safavian, D., and Goring, D.R. (2013). Secretory activity is rapidly induced in stigmatic papillae by compatible pollen, but inhibited for self-incompatible pollen in the Brassicaceae. *PLoS One* 8, e84286. <https://doi.org/10.1371/journal.pone.0084286>.
39. Indriolo, E., and Goring, D.R. (2014). A conserved role for the ARC1 E3 ligase in Brassicaceae self-incompatibility. *Front. Plant Sci.* 5, 181. <https://doi.org/10.3389/fpls.2014.00181>.
40. Indriolo, E., Safavian, D., and Goring, D.R. (2014). The ARC1 E3 Ligase Promotes Two Different Self-Pollen Avoidance Traits in *Arabidopsis*. *Plant Cell* 26, 1525–1543. <https://doi.org/10.1105/tpc.114.122879>.
41. Brillada, C., Teh, O.K., Ditungou, F.A., Lee, C.W., Klecker, T., Saeed, B., Furlan, G., Zietz, M., Hause, G., Eschen-Lippold, L., et al. (2021). Exocyst subunit Exo70B2 is linked to immune signaling and autophagy. *Plant Cell* 33, 404–419. <https://doi.org/10.1093/plcell/koaa022>.
42. Ji, C., Zhou, J., Guo, R., Lin, Y., Kung, C.H., Hu, S., Ng, W.Y., Zhuang, X., and Jiang, L. (2020). AtNBR1 Is a Selective Autophagic Receptor for AtExo70E2 in *Arabidopsis*. *Plant Physiol.* 184, 777–791. <https://doi.org/10.1104/pp.20.00470>.
43. Bodemann, B.O., Orvedahl, A., Cheng, T., Ram, R.R., Ou, Y.H., Formstecher, E., Maiti, M., Hazelett, C.C., Wauson, E.M., Balakireva, M., et al. (2011). RalB and the exocyst mediate the cellular starvation response by direct activation of autophagosome assembly. *Cell* 144, 253–267. <https://doi.org/10.1016/j.cell.2010.12.018>.
44. Ding, Y., Robinson, D.G., and Jiang, L. (2014). Unconventional protein secretion (UPS) pathways in plants. *Curr. Opin. Cell Biol.* 29, 107–115. <https://doi.org/10.1016/j.ceb.2014.05.008>.
45. Rueden, C.T., Schindelin, J., Hiner, M.C., DeZonia, B.E., Walter, A.E., Arena, E.T., and Eliceiri, K.W. (2017). ImageJ2: ImageJ for the next generation of scientific image data. *BMC Bioinf.* 18, 529. <https://doi.org/10.1186/s12859-017-1934-z>.
46. Liu, H., Ding, Y., Zhou, Y., Jin, W., Xie, K., and Chen, L.L. (2017). CRISPR-P 2.0: An Improved CRISPR-Cas9 Tool for Genome Editing in Plants. *Mol. Plant* 10, 530–532. <https://doi.org/10.1016/j.molp.2017.01.003>.
47. Xie, K., Minkenberg, B., and Yang, Y. (2015). Boosting CRISPR/Cas9 multiplex editing capability with the endogenous tRNA-processing system. *Proc. Natl. Acad. Sci. USA* 112, 3570–3575. <https://doi.org/10.1073/pnas.1420294112>.
48. Dai, C., Li, Y., Li, L., Du, Z., Lin, S., Tian, X., Li, S., Yang, B., Yao, W., Wang, J., et al. (2020). An efficient *Agrobacterium*-mediated transformation method using hypocotyl as explants for *Brassica napus*. *Mol. Breeding* 40, 96. <https://doi.org/10.1007/s11032-020-01174-0>.
49. Zhang, X., Henriques, R., Lin, S.S., Niu, Q.W., and Chua, N.H. (2006). *Agrobacterium*-mediated transformation of *Arabidopsis thaliana* using the floral dip method. *Nat. Protoc.* 1, 641–646. <https://doi.org/10.1038/nprot.2006.97>.
50. Ketelaar, T., Voss, C., Dimmock, S.A., Thumm, M., and Hussey, P.J. (2004). *Arabidopsis* homologues of the autophagy protein Atg8 are a novel family of microtubule binding proteins. *FEBS Lett.* 567, 302–306. <https://doi.org/10.1016/j.febslet.2004.04.088>.
51. Sassi, M., Ali, O., Boudon, F., Cloarec, G., Abad, U., Cellier, C., Chen, X., Gilles, B., Milani, P., Friml, J., et al. (2014). An auxin-mediated shift toward growth isotropy promotes organ formation at the shoot meristem in *Arabidopsis*. *Curr. Biol.* 24, 2335–2342. <https://doi.org/10.1016/j.cub.2014.08.036>.
52. Riglet, L., Rozier, F., Kodera, C., Bovio, S., Sechet, J., Fobis-Loisy, I., and Gaude, T. (2020). KATANIN-dependent mechanical properties of the stigmatic cell wall mediate the pollen tube path in *Arabidopsis*. *Elife* 9, e57282. <https://doi.org/10.7554/eLife.57282>.
53. Rozier, F., Riglet, L., Kodera, C., Bayle, V., Durand, E., Schnabel, J., Gaude, T., and Fobis-Loisy, I. (2020). Live-cell imaging of early events following pollen perception in self-incompatible *Arabidopsis thaliana*. *J. Exp. Bot.* 71, 2513–2526. <https://doi.org/10.1093/jxb/eraa008>.

STAR★METHODS

KEY RESOURCES TABLE

| REAGENT or RESOURCE | SOURCE | IDENTIFIER |
|--|----------------------------|-----------------------------------|
| Antibodies | | |
| Anti-Exo84c | This study | N/A |
| Anti-GFP | Biorbyt | Cat# Orb323045 |
| Anti-Actin | BBI Life Sciences | Cat# D110007 |
| HRP-conjugated goat anti-mouse | Yeasen | Cat# 33201ES60; RRID: AB_10015289 |
| HRP-conjugated goat anti-rabbit | BBI Life Sciences | Cat# D110058 |
| Bacterial and virus strains | | |
| <i>Agrobacterium tumefaciens</i> GV3101 | TransGen Biotech | N/A |
| <i>E. coli</i> DH5 α (Trans-T1) | TransGen Biotech | Cat# CD501-1 |
| <i>E. coli</i> BL21 (DE3) | TransGen Biotech | Cat# CD601-2 |
| Chemicals, peptides, and recombinant proteins | | |
| Aniline blue | Sinopharm Chemical Reagent | Cat# 71003644 |
| Cycloheximide | MedChemExpress | Cat# 121653 |
| Concanamycin A | APEX BIO | Cat# A8633 |
| Lanolin | Macklin | Cat# L812568 |
| pET28a Exo84c | This study | N/A |
| pMDC43 SLR1:secGFP | This study | N/A |
| pCL112 nYFP-Exo84c | Zhang et al. ¹² | N/A |
| pCL113 cYFP-Exo70A1 | This study | N/A |
| pCL113 cYFP-Sec6 | This study | N/A |
| pMDC83 Exo84c-mCherry | This study | N/A |
| pMDC43 GFP-Exo70A1 | This study | N/A |
| pUBC Sec6p:Sec6-GFP | This study | N/A |
| pMDC43 Exo70A1:GFP-Exo70A1 | This study | N/A |
| Critical commercial assays | | |
| RevertAid First Strand cDNA Synthesis Kit | Thermo Fisher Scientific | Cat# K1622 |
| Universal DNA Purification Kit | TIANGEN | Cat# DP214 |
| TIANprep Rapid Mini Plasmid Kit | TIANGEN | Cat# DP105 |
| SV Total RNA Isolation System | Promega | Cat# Z3100 |
| LR Clonase II Enzyme Mix | Invitrogen | Cat# 11791020 |
| Smart Assembly Cloning Kit | Smart-Lifesciences | Cat# SC00450 |
| Experimental models: Organisms/strains | | |
| <i>B. napus</i> : S70 | Chen et al. ¹⁶ | N/A |
| <i>B. napus</i> : Westar | Zhang et al. ¹⁴ | N/A |
| <i>A. thaliana</i> : Col-0 | ABRC | N/A |
| <i>A. thaliana</i> : <i>exo84c</i> | Salk collection | N/A |
| <i>A. thaliana</i> : <i>exo84c/Exo84cpro</i> : Exo84c-GFP | Zhang et al. ¹² | N/A |
| <i>A. thaliana</i> : SI-Col-0 | Zhang et al. ²¹ | N/A |
| Oligonucleotides | | |
| BnExo84c sgRNA-1F: TAGGTCTCC CTGCATCACCAGGTTTTAGAGCTAGAA | This study | N/A |
| BnExo84c sgRNA-1R: ATGGTCTCA GCAGATGAGTCATGCACCAGCCGGGAA | This study | N/A |

(Continued on next page)

Continued

| REAGENT or RESOURCE | SOURCE | IDENTIFIER |
|--|-----------------------------|------------|
| BnExo84c sgRNA-2F: TAGGTCTCCT TAAAGAGAACGGTTTTAGAGCTAGAA | This study | N/A |
| BnExo84c sgRNA-2R: ATGGTCTCA TTAACCAAACGGTGCACCAGCCGGGAA | This study | N/A |
| BnExo84c Hi-TOM-F: GGAGTGAGTA CGGTGTGCCTCGTGCAKGATCTGAT GTCTGGAC | This study | N/A |
| BnExo84c Hi-TOM-R: GAGTTGGAT GCTGGATGGGAATGTCAATCTTCTC CAGGAACTC | This study | N/A |
| Exo84c pep-F: ATGGAGAGCAGCGAG GAAGAC | This study | N/A |
| Exo84c pep-R: AGACTTTGGATC GGTACTTCATTAGGC | This study | N/A |
| Sec6 CDS-F: ATGATGGTCTGAAGATCTTG GTGTG | This study | N/A |
| Sec6 CDS-R: AGTGAGTTTTCGCCACA TAGATCC | This study | N/A |
| Sec6 promoter-F: CAGTTTGTG GAGTATTTAGAAAGAATTTCG | This study | N/A |
| Sec6 promoter-R: CTTGCTA AATCACCTTATTACGAACTCC | This study | N/A |
| Exo70A1 CDS-F: ATGGCTGTTGATAGCAGAATGG | This study | N/A |
| Exo70A1 CDS-R: TTACCGGCGTGGTTCATTTCATA | This study | N/A |
| Exo70A1 promoter-F: GTTTTGGAATCGCGGCTGC | This study | N/A |
| Exo70A1 promoter-R: GGCGAATTCCAAAAGCTGGAGA | This study | N/A |
| SLR1 promoter-F: GGATCCCTGGGTCATTGCT | This study | N/A |
| SLR1 promoter-R: CTCTCTC TTCACCACTTTAATTTCTATGC | This study | N/A |
| secGFP-F: ATGAAGAC TAATCTTTTCTCTTTCTCA | This study | N/A |
| secGFP-R: TTACAAATCC TCCTCAGAGATAAGCTTCTGCTC | This study | N/A |
| Software and algorithms | | |
| ImageJ | Rueden et al. ⁴⁵ | J2 |
| Prism | Alliance Development Group | V8.0 |
| Other | | |
| Table S2 (Gene accession numbers) | This study | N/A |

RESOURCE AVAILABILITY

Lead contact

Further information and requests for resources and reagents should be directed to and will be fulfilled by the lead contact, Pengwei Wang (wangpengwei@mail.hzau.edu.cn).

Materials availability

Materials generated in this study are available upon reasonable requests.

Data and code availability

- All data reported in this paper will be shared by the [lead contact](#) upon request.
- This paper does not report original code.
- Any additional information required to reanalyze the data reported in this paper is available from the [lead contact](#) upon request.

EXPERIMENTAL MODEL AND STUDY PARTICIPANT DETAILS

Experiments performed with *Brassica napus* plants were done using ‘S70’ (a self-incompatible allotetraploid line with $S_{1300}S_6$ haplotype) and ‘Westar’ (a self-compatible allotetraploid line with S_7S_6 haplotype) cultivars. All *B. napus* plants were grown in a greenhouse under a light intensity of $100 \mu\text{mol m}^{-2} \text{s}^{-1}$ with a 16/8 h light/dark photoperiod at 22°C, or in the transgenic plant field at Huazhong Agricultural University. The *Arabidopsis thaliana* seeds of transfer DNA insertion lines for *exo84c* (SALK_011569) were obtained from the Nottingham Arabidopsis Stock Center, and the transgenic self-incompatible Arabidopsis in Col-0 background has been generated previously.²¹ Arabidopsis plants were grown in a greenhouse at 22°C with 16 h of light and 8 h of darkness.

METHOD DETAILS

Transmission Electron Microscopy

The *B. napus* stigmas were harvested at 30 min after compatible or incompatible pollination, and were vacuum-infiltrated and pre-fixed in a solution of 2.5% glutaraldehyde adjusted to pH 7.4 with 0.1 M phosphate buffer. Then the samples were post-fixed in 2% OsO_4 , followed by dehydration and embedding in epoxy resin and SPI-PON 812 (SPI Supplies, West Chester, PA, USA). Ultra-thin sections were obtained using a Leica UC6 ultramicrotome and were stained with uranyl acetate and lead citrate. For TEM imaging, a Hitachi H-7650 transmission electron microscope was used at 80 kV.

Brassica napus transformation

The conserved synthetic guide RNA sequences from exons of BnExo84c A08 and C08 genes were designed with the web tool CRISPR-P2.0 (<http://crispr.hzau.edu.cn/CRISPR2/>).⁴⁶ Two single guide RNAs (sgRNA) were chosen to target the two copies of BnExo84c. The sgRNA cassette was finally cloned into the pRGE32 vector.⁴⁷ The *Bnexo84c* mutants were generated by *Agrobacterium tumefaciens* (GV3101) mediated *B. napus* transformation.⁴⁸ CRISPR/Cas9 induced sequence mutations on different BnExo84c copies were detected using the high-throughput tracking of mutations method (Hi-TOM). Degenerate primers for amplifying the flanking sequence of the target were designed according to the reference sequences of the two BnExo84c copies.

Arabidopsis thaliana transformation

The protein secretion marker secGFP²³ driven by the stigma-specific SLR1 promoter (ref) was cloned into pMDC43 vector through Gibson assembly. The 1.5-kb Sec6 promoter fused to its full-length Sec6 CDS (without stop codon) was cloned into pUBC vector to generate Sec6pSec6:GFP. The coding sequence of Exo70A1 was cloned into pMDC43 vector driven by 35S promoter, then the 35S promoter was substituted by the 2-kb Exo70A1 promoter to generate Exo70A1pGFP-Exo70A1. All expression constructs were transformed into *Agrobacterium tumefaciens* GV3101 by electroporation. A stable Arabidopsis Col-0 line with pollen labeled by Lat52RFP-HDEL was generated and crossed with SI-Col-0 to observe SC and SI pollination process. Stable transgenic Arabidopsis lines were generated by floral dipping.⁴⁹

Production of anti-Exo84c polyclonal antibodies

An Exo84c specific (corresponding to amino acids 1–130 of *Arabidopsis thaliana* Exo84c) peptide was cloned into pET28a plasmid (Novagen, Darmstadt, Germany) that carries an N-terminal His-tag. The expression of recombinant proteins was performed using the *Escherichia coli* BL21 strain and purified with nickel agarose beads (BBI Life Sciences, China). Purified proteins were dialyzed in PBS +10% glycerol overnight at 4°C. Polyclonal antibodies were raised in 4-week-old mice. 50 μg antigen was used for each boost, and a total of 4 boosts over 2 months were performed. Antiserum was collected 10 days after the final boost.⁵⁰ Approval was granted by the Animal Experimental Ethical Inspection of Laboratory Center at Huazhong Agricultural University.

Protein extraction and immunoblot analysis

Total proteins used for immunoblot analysis were extracted from *B. napus* mature buds or 10-day-old Arabidopsis seedlings. The samples were ground in liquid nitrogen and mixed with equal volumes of $2 \times$ SDS buffer with 50 mM Tris-HCl, 40 mM NaCl, 10 mM MgCl_2 , 5 mM EDTA and 5 mM DTT. The mixture was incubated at 98°C for 10 min and centrifuged to collect the supernatant. The total protein samples were loaded at appropriate amounts on 5% stacking gel and separated on a 10% or 12% SDS-PAGE separating gel. The proteins were then transferred to a nitrocellulose membrane after electrophoresis. The membrane was probed with primary antibody (1:500 for anti-Exo84c; 1:1000 for anti-Actin, BBI Life sciences; 1:2000 for anti-GFP, Biorbyt) and a horseradish peroxidase (HRP)-conjugated goat anti-mouse/rabbit secondary antibody (Yeasen, used at 1:5000; BBI Life sciences, used at 1:5000) at room temperature.

Chemical treatment

For treatment of the stigmatic papilla cells, lanolin containing 25 μ M Conc A or/and 0.5 mM wortmannin was applied around the style.^{51,52} For protein degradation rate analysis, 10-day-old Arabidopsis seedlings were treated in liquid 1/2 MS medium with 50 μ M cycloheximide or 50 μ M cycloheximide together with 1 μ M Conc A.

Pollination assay and silique clearing

Flower buds from *B. napus* and Arabidopsis were emasculated one day before anthesis. The pistils were cut at the peduncle 24 h after pollination and fixed in Carnoy's fixative (ethanol: acetic acid = 3:1) for 2 h. Then the pistils were softened in 1 M NaOH at 60°C for 1 h and stained with 0.01% (w/v) aniline blue for 2.5 h in 2% (w/v) K_3PO_4 . The samples were mounted onto a microscopic slide glass by placing the cover glass over the pistils and observed under a fluorescence microscope (Leica DMi8).

For silique clearing, the Arabidopsis siliques were collected 12 days post-pollination and submerged in 75% ethanol for 3–5 days. Images were obtained using a stereo fluorescence microscope (Leica M205 FA).

Pollen hydration assay

Pistils used for this assay were emasculated one day before anthesis. The pistils were cut at the peduncle 24 h after emasculating and settled on 0.8% (w/v) agarose which was covered on slides. One anther was picked each time and gently swiped onto the stigma under a stereomicroscope (Leica M205 FA) to ensure an appropriate amount of pollen grains landing on the papilla cells. The process of compatible or incompatible pollen hydration process was captured using an upright fluorescence microscope (Leica DM6B). The pollen hydration rate was estimated by calculating the ratio between the length and width of each pollen grain.⁵³

Confocal microscopy and image analysis

Emasculated Arabidopsis flowers were pollinated with compatible or incompatible pollen expressing Lat52RFP-HDEL. The stigmas were clipped off the pistils and mounted on a glass slide. Images were collected using a laser scanning confocal microscope (Leica TCS SP8) with a 63 \times oil-immersion objective lens using the Leica PMT detector. The excitation/emission wavelengths for GFP and RFP are 488 nm/505–550 nm and 552 nm/590–640 nm, respectively. The fluorescence intensity and band intensity (in western blot assay) were measured using ImageJ.

QUANTIFICATION AND STATISTICAL ANALYSIS

Bar graphs with dots were performed with Prism. Details of statistical evaluations and the numbers of samples are provided in the figure legends or the figures.